Electrostatics, hydration, and proton transfer dynamics in the membrane domain of respiratory complex I

Ville R. I. Kaila[a,b,1], Mårten Wikström[c], and Gerhard Hummer[b,d,1]

[a]Department Chemie, Technische Universität München, D-85748 Garching, Germany; [b]Laboratory of Chemical Physics, National Institute of Diabetes and Digestive and Kidney Diseases, National Institutes of Health, Bethesda, MD 20892-0520; [c]Helsinki Bioenergetics Group, Institute of Biotechnology, University of Helsinki, FI-00014 Helsinki, Finland; and [d]Department of Theoretical Biophysics, Max Planck Institute of Biophysics, 60438 Frankfurt am Main, Germany

Edited by Harry B. Gray, California Institute of Technology, Pasadena, CA, and approved April 1, 2014 (received for review October 16, 2013)

Complex I serves as the primary electron entry point into the mitochondrial and bacterial respiratory chains. It catalyzes the reduction of quinones by electron transfer from NADH, and couples this exergonic reaction to the translocation of protons against an electrochemical proton gradient. The membrane domain of the enzyme extends ∼180 Å from the site of quinone reduction to the most distant proton pathway. To elucidate possible mechanisms of the long-range proton-coupled electron transfer process, we perform large-scale atomistic molecular dynamics simulations of the membrane domain of complex I from *Escherichia coli*. We observe spontaneous hydration of a putative proton entry channel at the NuoN/K interface, which is sensitive to the protonation state of buried glutamic acid residues. In hybrid quantum mechanics/classical mechanics simulations, we find that the observed water wires support rapid proton transfer from the protein surface to the center of the membrane domain. To explore the functional relevance of the pseudosymmetric inverted-repeat structures of the antiporter-like subunits NuoL/M/N, we constructed a symmetry-related structure of a possible alternate-access state. In molecular dynamics simulations, we find the resulting structural changes to be metastable and reversible at the protein backbone level. However, the increased hydration induced by the conformational change persists, with water molecules establishing enhanced lateral connectivity and pathways for proton transfer between conserved ionizable residues along the center of the membrane domain. Overall, the observed water-gated transitions establish conduits for the unidirectional proton translocation processes, and provide a possible coupling mechanism for the energy transduction in complex I.

biological energy conversion | proton pumping | Grotthuss mechanism | QM/MM

Complex I, or NADH:ubiquinone oxidoreductase, is an enzyme crucial for biological energy conversion. By transferring electrons from reduced NADH to quinone (Q), it functions as a primary entry point for electrons into the mitochondrial and bacterial respiratory chains (1, 2). Complex I couples the Q reduction to translocation of three to four protons across the mitochondrial or bacterial membrane (3, 4), thus contributing to the electrochemical proton-motive force subsequently used for synthesis of ATP by F_oF_1-ATPase and for active transport of solutes (5).

Complex I is a large (550–980 kDa) L-shaped enzyme, which consists of a hydrophilic domain located in the mitochondrial matrix/bacterial cytoplasm, and a membrane domain, embedded in the mitochondrial inner membrane/bacterial cytoplasmic membrane (1, 2). Its 14 core subunits are evolutionarily conserved in bacteria and eukaryotes (1), with over 20 additional subunits in higher organisms (6). The hydrophilic domain provides an electron transfer chain from NADH via a flavine mononucleotide and eight to nine iron-sulfur centers to Q, located at the end of this chain (Fig. 1*A*) (7, 8). Leakage from this electron transfer pathway is a likely source of mitochondrial reactive oxygen species (9) associated with neurodegenerative diseases and aging.

The proton-translocating membrane domain of complex I comprises three antiporter-like subunits, NuoN, NuoM, and NuoL (*Escherichia coli* naming), which are connected to the hydrophilic domain by the NuoA/J/K/H subunits (10, 11). The antiporter-like subunits are homologous to each other as well as to, for example, Mrp (multiresistance and pH adaptation) Na^+/H^+-antiporters and certain hydrogenases (12). The antiporter-like subunits have an intrinsic sequence identity of ∼20%, but an even more evident structural homology: the transmembrane (TM) helices 4–8 and 9–13 can be structurally superimposed (Fig. 1*B*). These subunits also contain several crucial residues for the proton translocation process (Fig. 1*C*): a conserved Lys-Glu (or Asp in NuoL) ion pair in TM helices 5/7a, and one or two other conserved lysines, have been confirmed by site-directed mutagenesis experiments to be crucial for the proton translocation process (1, 2) (Table S1). During the completion of this study, a new X-ray structure of the intact complex I from *Thermus thermophilus* was released (13). The structure reveals that the NuoH subunit (Nqo8 in *T. thermophilus*) has structural resemblance to the TM helix segment 4–8 of the antiporter-like NuoN/M/L subunits (13), and may thus also be involved in the proton-pumping machinery. A detailed comparison of key regions of the *Escherichia coli* and *T. thermophilus* membrane domains is shown in Fig. S1.

Interestingly, mutation of conserved residues in the NuoL subunit, ∼180 Å away from the hydrophilic domain, leads to loss of the Q-reductase activity (1, 2) (Table S1). Although expected for a fully reversible proton-coupled electron transfer machine, this tight coupling imposes severe mechanistic demands. Remarkably, after deletion of subunits equivalent to NuoL and NuoM, the apparent pumping stoichiometry was reduced by about one-half (14). The putative proton transfer pathways through the membrane domain are distant from the redox-active

Significance

Using large-scale classical and quantum simulations, we elucidate key aspects of the molecular function of complex I, a protein central to biological energy conversion. Complex I serves as the primary electron entry point into the mitochondrial and bacterial respiratory chains and operates as a redox-coupled proton pump. Our simulations suggest that transient water chains establish highly efficient pathways for proton transfer. Our findings form a basis for understanding long-range energy conversion in complex I, and mechanistic similarities to other redox-driven proton-pumps, such as cytochrome *c* oxidase and bacteriorhodopsin.

Author contributions: V.R.I.K., M.W., and G.H. designed research; V.R.I.K. performed research; V.R.I.K., M.W., and G.H. analyzed data; and V.R.I.K., M.W., and G.H. wrote the paper.

The authors declare no conflict of interest.

This article is a PNAS Direct Submission.

[1]To whom correspondence may be addressed. E-mail: ville.kaila@ch.tum.de or gerhard.hummer@biophys.mpg.de.

This article contains supporting information online at www.pnas.org/lookup/suppl/doi:10.1073/pnas.1319156111/-/DCSupplemental.

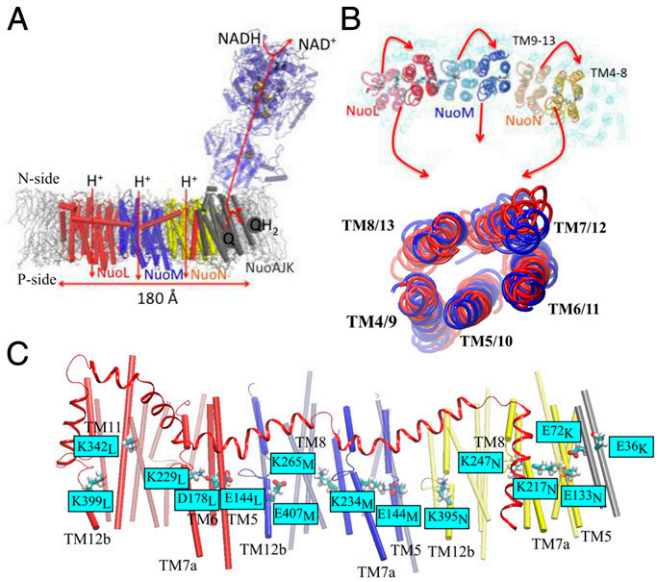

Fig. 1. Structure and internal symmetry of complex I from *E. coli*. (*A*) Membrane (PDB ID: 3RKO) and hydrophilic domains (PDB ID: 2FUG) of complex I embedded in a lipid membrane. The antiporter-like subunits NuoN, NuoM, and NuoL are shown in yellow, blue, and red, respectively. (*B*) TM helix segments 4–8 (blue) and 9–13 (red) in NuoN/M/L structurally superimposed. TM helices 4–6 and 9–11 have high structural similarity, whereas TM helices 7–8, and 12–13 are in a different conformation. (*C*) Position of key residues in the membrane domain of complex I. The amphipathic HL helix (red) lies parallel to the membrane plane, and contacts all three antiporter-like subunits.

groups mediating electron transfer through the hydrophilic domain (10). As a consequence, the proton-coupled electron transfer in complex I is expected to differ mechanistically from that in other systems, such as ribonucleotide reductase, an enzyme involved in synthesis of DNA from RNA, where the proton and the electron are transferred concertedly along a pathway of conserved residues (15, 16). In contrast, in complex I the electron and proton transfers are separated both kinetically and spatially. To explain this long-range coupling, both "direct" (redox-driven) and "indirect" (conformational-driven) mechanisms have been suggested, but the molecular principles of these mechanisms remain elusive (1, 2, 4, 17–22).

Complex I has been suggested to undergo conformational changes, which may drive the proton-translocation process (11, 23). Superimposing the TM helix segments of NuoN, NuoM, and NuoL suggests that TM helices 4–6/9–11 are structurally in a similar conformation, whereas the TM helices 7–8/12–13 have a different tilting angle relative to the membrane normal (Fig. 1*B*). In terms of its evolutionary homology to antiporters, this internal symmetry would suggest that the two segments are in different conformational states with connectivity to different sides of the membrane, in analogy to what has been observed for carrier-type transporters (24).

To gain further insight into the long-range coupling mechanism, we study here the dynamics of the membrane domain of complex I from *E. coli* by large-scale atomistic molecular dynamics (MD) simulations, hybrid quantum mechanics/molecular mechanics (QM/MM) approaches, and continuum electrostatics calculations. Our simulations, both in the state of the crystal structure and in a putative alternate-access state with inverted symmetry established by harmonic restraints, give molecular insight into the structural dynamics and coupling of key residues involved in the proton translocation process. Instead of large-scale conformational changes associated with traditional transporter function, we show here that extensive changes in internal hydration establish the changes in protonic access required for pumping. With these hydration changes found to be strongly coupled to the charge states of conserved titratable residues, and their charge states in turn coupled to each other, internal water thus emerges as the key element in the redox-coupled proton translocation process that connects the extensive network of buried ionizable residues with each other and with the surfaces.

Results

Proton Uptake Channels. In an unrestrained MD simulation of the membrane domain of complex I, we observed spontaneous hydration of the initially dry NuoN/NuoK interface at 220–240 ns (Fig. 2). The resulting water chain established hydrogen-bond connectivity between the N-side of the membrane and the buried

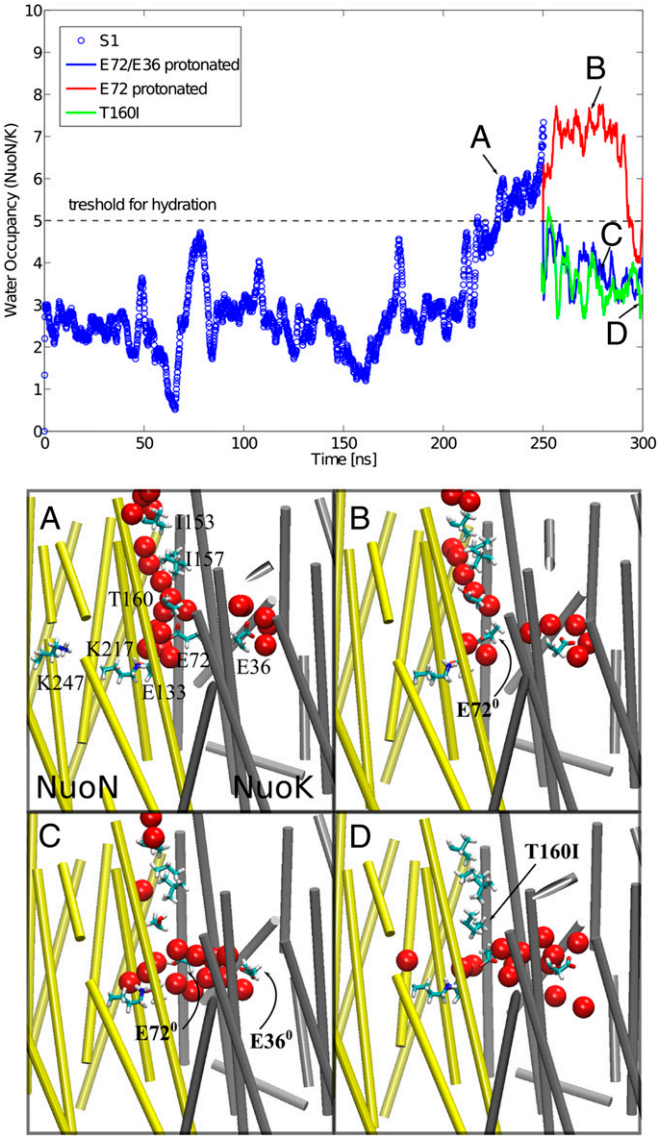

Fig. 2. Hydration of the proton uptake channel in complex I at the NuoN/NuoK interface. (*Upper*) Water occupancy showing a spontaneous influx at ~220 ns (symbols). Drying is induced by neutralization of both Glu-36_K and Glu-72_K (blue line), but not of Glu-72_K alone (red line), and by a $T160_N$I mutation (green line), starting from the hydrated configuration at 250 ns, and simulated for 50 ns. (*Lower*) MD snapshots of (*A*) S_1 state, (*B*) after protonation of Glu-72_K ($E72^0$), (*C*) after protonation of Glu-36_K and Glu-72_K ($E36^0$, $E72^0$), and (*D*) in T160I mutant, as indicated in the *Upper* panel.

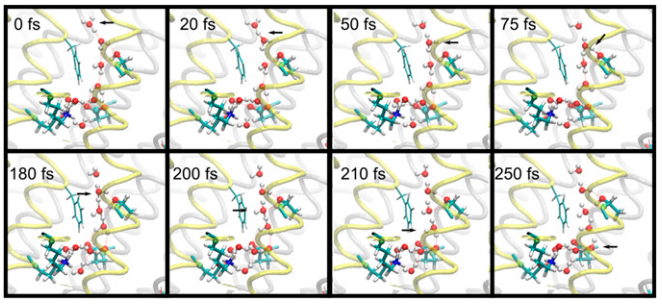

Fig. 3. Snapshots of the QM/MM simulation of proton uptake from the N-side of the membrane along the water chain of Fig. 2*A* to Glu-72$_K$. Arrows indicate the locations of the protonic defect. The dynamics of the hydrogen-bonded network is shown in Fig. S2 and Movie S1.

residues Glu-72$_K$ and Glu-36$_K$ (Fig. 2*A*). The opening of this water conduit at the N-side of the membrane is lined by positively charged residues at the channel opening, followed by a hydrophobic gate before reaching Glu-72$_K$ and Glu-36$_K$ (Fig. 2*A*). Glu-72$_K$ at the center of the membrane domain serves as a bifurcation point, with chains of ionizable residues and water molecules continuing both toward NuoN and toward NuoK.

The formation of the water chain is tightly coupled to the protonation state of conserved ionizable residues at the center of the membrane domain. After we protonated both Glu-72$_K$ and Glu-36$_K$ in the hydrated configuration obtained at the end of the 250-ns simulation, the water chain destabilized and disassembled on a nanosecond timescale (Fig. 2*C*). In contrast, the water chain persisted for the entire 50-ns simulation when only Glu-72$_K$ was protonated (Fig. 2*B*). These findings indicate that the reversibly formed water chain and the buried carboxylates at the center of the membrane domain may function as proton transfer mediators, consistent with electrostatics calculations and site-directed mutagenesis experiments described below, and similar to what has been suggested for Glu-242 in cytochrome *c* oxidase (C*c*O) (25–27). To deliver protons, water may provide a reversible molecular gate that opens when the glutamates are deprotonated, and closes in their neutral state.

Indeed, in hybrid QM/MM simulations we observed rapid proton transfer from the N-side of the membrane along the water chain to the conserved glutamates (Fig. 3 and Movie S1). We performed five independent QM/MM simulations of the uptake of a proton from the bulk region. Starting from a hydronium ion (H_3O^+) placed initially at the N-side opening, the proton diffused consistently within ~1 ps over a distance of ~11 Å to Glu-72$_K$, alternating between hydronium (H_3O^+) and Zundel ($H_5O_2^+$) structures in a Grotthuss-type fashion (28–30) (Fig. S2). The hydroxyl group of residue Thr-160$_N$ helped stabilize the water chain through hydrogen bonding, but did not participate directly in the proton transfer process. Despite transiently sharing a proton with a water molecule forming a Zundel structure (Fig. 3 and Movie S1), Thr-160$_N$ did not give up its proton during any of the transfer reactions.

Experiments also support a functional role of the transient water chain leading to Glu-72$_K$ and Glu-36$_K$: replacing these residues with untitratable glutamines strongly inhibits both pumping and the Q-reduction activity (Table S1), indicating that the residues are likely to be actively involved in the proton-uptake process. Structurally, these glutamates reside in close proximity (~5 Å) from each other, and Glu-72$_K$ is separated by only 4 Å from the Glu/Lys ion pair, suggesting that the protonation states of these residues are strongly coupled (see below). Amarneh and Vik (31) (Table S1) found the T160I$_N$ point mutation to decrease both Q-reduction activity and to inhibit proton pumping in the *E. coli* enzyme, although in contrast to the glutamates discussed above, T160 is not conserved in all species. Nevertheless, in the 50-ns classic MD simulation of the in silico-mutated T160$_N$I-model (simulation S$_9$) (Fig. 2*D*), initiated from the fully hydrated channel structure, we observed disassembly of the water chain within 1 ns, triggered by a rotation of the bulky hydrophobic side-chain of Ile-160$_N$ and blockage of the channel to the N-side of the membrane. This side-chain rotation most likely shields the charge of the buried carboxylates and may thus decrease the influx of water and, in turn, of protons into the protein interior. Although the NuoH subunit is missing from the membrane structure of complex I from *E. coli*, we find that the structure of the NuoN/K interface remains nearly unchanged relative to the complete structure of complex I (Fig. S1). In particular, the three glutamates at the interface are conserved, suggesting that the hydration effects observed here at the NuoN/K interface also occur in the complete structure of complex I.

Fig. 4 shows the proton transfer pathways inferred by Efremov and Sazanov (10) as "likely" and "less likely" on the basis of their X-ray structure. These pathways are compared with the hydration pattern at the end of the 250-ns unrestrained MD simulation. Overall, we find remarkable consistency, with putative pathways of Efremov and Sazanov (10) showing significant local hydration, with the possible exception of the "likely" proton access pathway in NuoL (where the "less likely" pathway shows more significant hydration), and the exit pathways in NuoN and

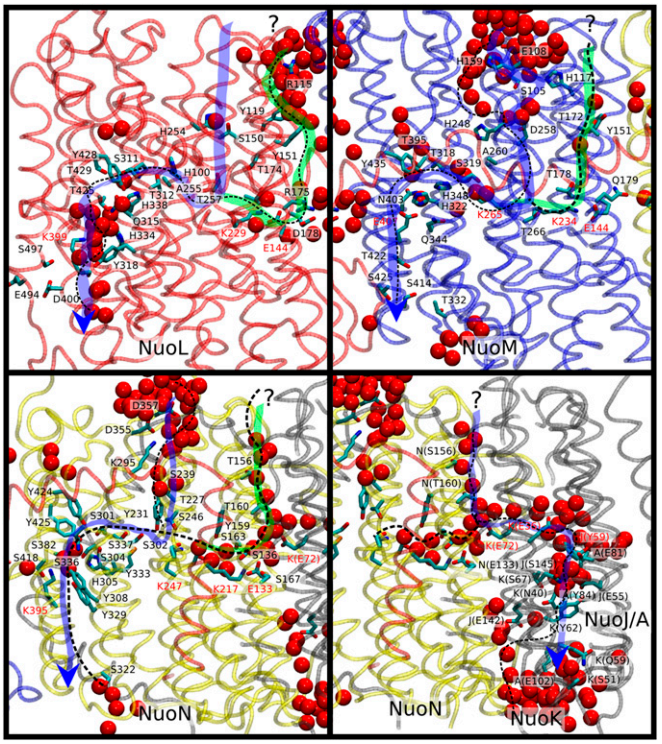

Fig. 4. Putative proton transfer pathways in complex I from the N-side (top of the subunit structures) to the P-side (bottom). The figure shows the proton transfer pathways suggested by Efremov and Sazanov (10), and relates them to the water occupancy obtained at the end of the 250-ns unrestrained MD simulation (see main text). Water molecules within a radius of 6 Å from the listed residues are shown in van-der-Waals representation (in red). The likely and less likely proton pathways suggested in Efremov and Sazanov (10) are indicated with blue and green lines, respectively, the latter being marked in addition with "?". The proton pathways indicated by the current simulations are shown as black dashed lines. Crucial charged residues according to Efremov and Sazanov (10) are labeled in red. The observed water density coincides with the alternate proton pathways of Efremov and Sazanov (10) in all subunits.

NuoM (with gaps in hydration). Most importantly, the reversibly hydrated, proton-conducting water wire leading to Glu-72_K identified and characterized here superimposes nicely with a pathway proposed by Efremov and Sazanov (10). The hydration pattern shown in Fig. 4 also suggests possible pathways from Glu-72_K to the N-side, either proceeding into the N subunit or directly along a water wire entering from the N-side toward Glu-72_K at the N/K interface. The observed hydration patterns thus provide further guidance for the experimental and computational delineation of the complete proton transfer network in complex I.

Conformational Changes in Antiporter-Like Subunits. Structural studies (10, 11, 23) suggested that complex I may undergo significant motion, possibly linked to proton-access alternation of the antiporter-like subunits. To study how an alternate-access state may induce activation of the proton pump, we performed a 150-ns MD simulation in a putative alternate access state, motivated by the evolutionary homology to antiporters and created by imposing the antiporter symmetry (24) onto the backbone. We restrained the two repeats TM 4–8 and 9–13 of NuoN related by a pseudotwo-fold symmetry axis (10) to their respective superimposed symmetry-related structures (i.e., the backbone structure of TM 4–8 imposed to the backbone structure of TM 9–13 and vice versa) (*Materials and Methods*). As a result of the ∼2 Å rmsd conformational change imposed on the NuoN backbone (Fig. S3), the extent of the interior hydration increased significantly beyond that of the unrestrained MD simulation, having started from a dry initial structure. As in the unrestrained simulation, the water molecules entered from the N-side of the membrane through the NuoN/K interface, but then additionally formed a hydrogen-bonded wire connecting the central Lys/Glu ion pair with the conserved distal lysine residues at the other end of the NuoN subunit along a lateral pathway at the center of the membrane domain (Fig. 5). Site-directed mutagenesis experiments have implicated these and other nearby residues in proton pumping (Table S1).

Whereas only NuoN was driven to an alternate access state by imposing structural restraints on the two antiporter-like halves of NuoN, the induced increase in hydration extended beyond to the NuoM subunit (Figs. 5 and 6). Water molecules occupied regions near the central Lys/Glu ion pair, and the more distant lysine/glutamate residues at the other antiporter-like half of the NuoM subunit (TM 9–13) (Fig. 5). In the most distal NuoL subunit, the hydration increased to the same level in the unrestrained and restrained simulations, albeit faster in the latter. However, in contrast to the dry crystal structure, the distal Lys-399_L residue formed a hydrogen-bonded connectivity with the P-side of the membrane. Similarly to the observed NuoN–NuoM coupling, we found the wetting transition to propagate to the NuoL subunits when the internal helix symmetry of the TM helices 4–8 and 9–13 in NuoM was interchanged (simulation S_5) (Fig. S4). The cooperativity between the hydration states of neighboring subunits could help activate the proton pump by switching from a "dry" inactive to a "wet" active state primed to proton uptake from the N-side of the membrane.

The antiporter-like subunits thus appear to toggle reversibly between dry and wet hydration states, with only minimal structural changes of their backbones (Fig. S3). Such alternating hydration states, with minimal conformational changes, would indeed be expected to be even more suitable for active proton translocation than the more leakage-prone conformational dynamics associated with traditional antiporter function. Indeed, upon releasing the structural constraints in the alternate configurational state of the S_2 simulation, we found that the backbone structure relaxed back close to its unbiased state, as indicated by the drop in rmsd (Fig. S3, *Top*). This relaxation suggests that the initial bias induced a reversible change in the structure. By contrast, the increased hydration persisted on the

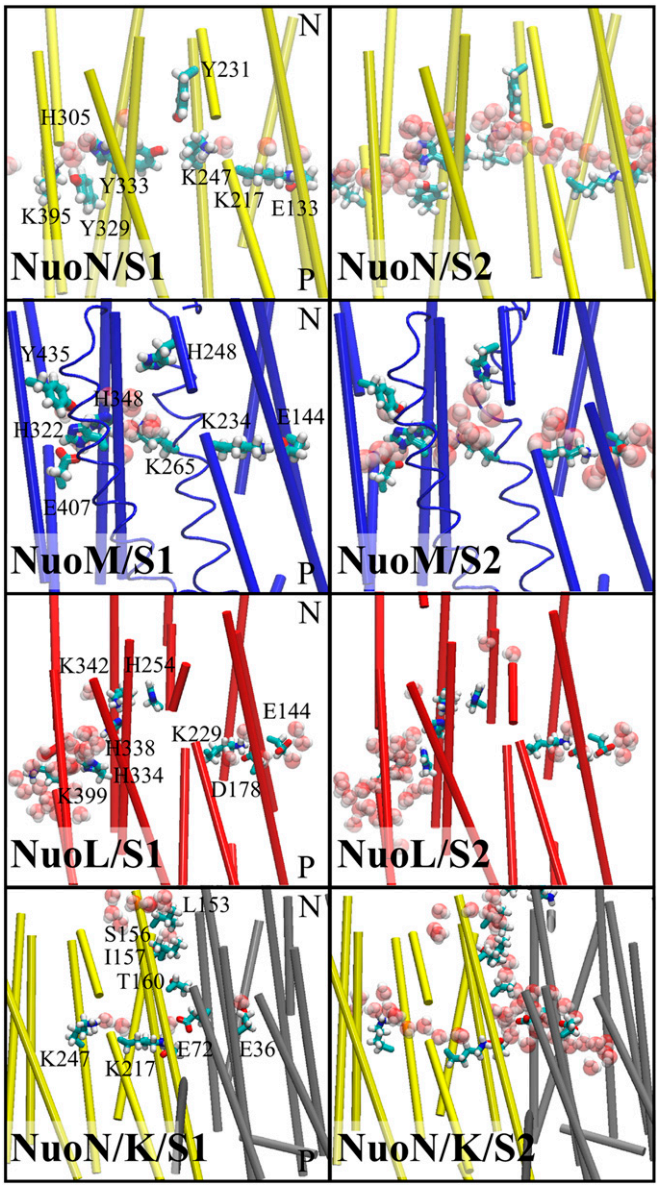

Fig. 5. Snapshots of two 150-ns MD simulations highlighting key residues in NuoN (yellow), NuoM (blue), NuoL (red), and NuoA/J/K (gray). In these side views of the membrane domain, the N-side is at the top. S_1 (*Left*) and S_2 (*Right*) represent the states obtained from the unrestrained simulation and after interchanging the internal helix symmetry of TM 4–8 and 9–13 in the NuoN subunit, respectively. Quasi-1D water chains, which provide hydrogen-bonded connectivity between key charged glutamic acid and lysine residues, are shown in van-der-Waals representation.

50-ns simulation timescale, even as the subunit backbone structures relaxed. Importantly, we did not observe any significant water escape from the protein back into bulk, as shown in Fig. 6. Our simulation data thus suggest that water molecules form a crucial element in this proton conduction pathway, similar to what has been suggested for C*c*O (25, 32, 33), as well as for the light-driven proton-pump bacteriorhodopsin (bR) (34). Our findings also directly support the hypothesis by Baradaran et al. (13) that water molecules may play an important role in providing protonic connectivity between key amino acids. Interestingly, the functional significance of transient hydration in the function of structurally related membrane transporters was recently also discussed by Li et al. (35).

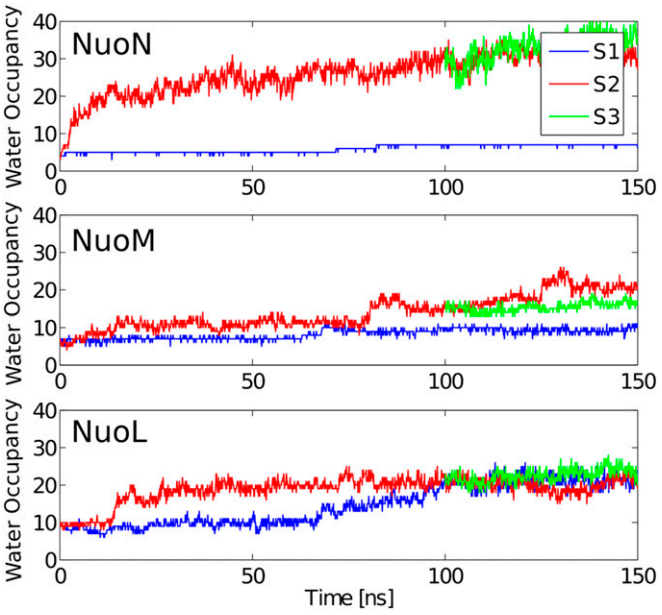

Fig. 6. Water occupancy in the S_1 (blue) and S_2 (red) states calculated within a radius of 5 Å from the side chains of charged residues at the center of the antiporter-like subunits, NuoN (*Top*), NuoM (*Middle*), NuoL (*Bottom*) (Table S5). The S_3 state (green) is obtained by releasing the structural constraints in the S_2 state at 100 ns. Transition to the S_2 state leads to influx of water molecules in all three subunits.

Electrostatic Coupling of Ionizable Residues. The results of continuum electrostatics calculations provide additional support for a possible functional role of the ionizable residues buried deeply in the membrane domain. Table 1 shows computed pK_a values of the conserved ionizable residues, obtained from an ensemble of structures along 100-ns segments of the MD trajectories. The calculated values suggest that most of these residues are in their charged states in the unrestrained state (S_1), but that the alternate extensively hydrated conformational state (S_2) leads to considerable shifts in computed pK_a values, and induced protonation changes in the central glutamic and lysine residues in the NuoN/K (Table 1). The calculations take into account the dielectric polarization of the medium, but may underestimate the inhomogeneous dielectric effects that result from the influx of water molecules. Despite these shortcomings, the S_2 state is predicted to lead to considerable changes in the electrostatic interaction energy between these charged residues, as shown in Table S2.

Table 1. Computed MD-averaged pK_a values of key residues in the S_1 and S_2 states

Subunit	Residue	S_1	S_2	S_2'
NuoK	Glu-36	D	15.7	9.3
	Glu-72	9.5	8.5	8.8
NuoN	Glu-133	D	D	**P**
	Lys-217	P	P	2.7
	Lys-247	16.0	3.0	2.7
	Lys-395	12.6	9.3	3.7
NuoM	Glu-144	D	D	**P**
	Lys-234	P	P	2.7
	Lys-265	11.1	9.8	10.8
	Glu-407	D	D	D*
NuoL	Asp-178	D	D	**P**
	Lys-229	P	P	2.6
	Lys-342	15.3	P	P
	Lys-399	P	P	16.5

D and P indicate residues that are deprotonated and protonated within the titration range of pH = 0–17, respectively. The S_2' state is obtained by biasing residues $E133_N$, $E144_M$, and $D178_L$ to protonate (boldface letters, P) in the Monte Carlo procedure.

*A pK_a of 18 is obtained for $E407_M$, when using an MD-averaged structures from a simulation with a protonated $E407_M$.

To obtain a better understanding of the intersubunit coupling, we analyzed the computed pK_a values upon protonation of the glutamates within the Lys-Glu ion pairs, which may be mediated by the water-chain to the N-side of the membrane. We found that protonation of the glutamic acid residues strongly decreased the pK_a of the respective lysine residue in the ion pairs. Deprotonation of the lysines could induce a proton displacement cascade within the subunit half-channels. However, our calculations further suggest that protonation of the glutamic acid in the Lys-Glu ion pair of NuoN alone may not induce a strong enough polarization to release a proton by the distal $Lys\text{-}395_N$ in the other half-channel of NuoN to the P-side of the membrane. In contrast, upon protonation of the glutamic acid in the Lys-Glu ion pair of NuoM, which may be driven by the cooperative intersubunit hydration effect, the computed pK_a of the distal $Lys\text{-}395_N$ strongly decreases from ~9–4, indicating that a proton is released to the P-side of the membrane. We observe analogous interaction energies between neighboring residues in the NuoM and NuoL subunits, which suggest that protonation of the carboxylates in NuoL may analogously induce a proton release from the NuoM subunit.

Discussion

The large-scale molecular simulations presented here suggest that the long-range energy propagation in complex I may function by charge-state–induced hydration transitions in the three antiporter-like subunits of the membrane domain. We observed cooperative hydration changes, which resulted in the formation of proton-conducting channels connecting the protein interior and surface, and possibly different membrane subunits. In addition, our electrostatics calculations showed that changes in hydration in turn induced changes in the energetically preferred protonation states. The electrostatic interactions between the buried ionizable residues are strong on a thermal energy scale, and the resulting coupling in the proton transfer network should be important for releasing protons to the P-side of the membrane. These findings directly support proton-pathways inferred from the recent X-ray crystal structures (10, 11) and numerous site-directed mutagenesis experiments, and help elucidate the molecular principles by which complex I catalyzes the long-range proton-pumping process.

The reaction cycle in complex I is initiated by reduction of Q, which results in a large charge imbalance (2, 4, 12, 20) that is expected to induce proton charge redistribution and in turn a cooperative hydration of the antiporter-like subunits. The newly released X-ray structure of complex I reveals that the Q-binding site is located in the hydrophilic NuoC (Nqo4) subunit above the interface with the membrane domains and is coupled to the latter by several charged residues within the NuoH (Nqo8) subunit. This "electrostatic wire," with interresidue separations between ionizable and polar amino acids of only 10–15 Å, could transmit events in the Q-binding site (13) to the membrane domain. However, a detailed characterization of the coupling between Q-reduction and proton pumping awaits further experimental and computational studies.

Although other proton-pumping enzymes, such as C*c*O (25, 32, 33) or bR (34), appear to use primarily local electrostatic changes induced by electron transfer or photo-excitation rather than conformational-induced changes, water molecules also seem to function as crucial "catalytic" elements in these systems (25, 32, 34). Despite large differences in the architecture of their

proton pumps, with bR related to receptors, C*c*O to NO reductases and other heme-copper oxidases, and complex I to antiporters, this finding suggests that water-gated transitions may provide a general mechanism for proton-pumping in biological energy conversion enzymes.

Materials and Methods

MD Simulations. The X-ray structure of the membrane domain of complex I from *E. coli* was obtained from the Brookhaven Protein Databank (PDB ID: 3RKO) (10). The protein was solvated in a POPC (1-palmitoyl-2-oleoyl-*sn*-glycero-3-phosphocholine) membrane, comprising 314 lipid molecules, 46,361 water molecules, and 55 Na^+ and 59 Cl^- ions, mimicking a 100-mM salt concentration (Fig. S5). The simulation system was comprised of 211,862 atoms, which were modeled using the CHARMM27 force field (36). Several MD simulations of 50–250 ns each (0.85 μs total) were performed at constant temperature ($T = 310$ K) and pressure ($P = 1$ atm), using a 2-fs timestep, and treating the long-range electrostatics with the Ewald approach. The simulations were performed using NAMD2 (37), and the results were analyzed in visual molecular dynamics (38). The details of the simulation setups are listed in Tables S3 and S4.

QM/MM Simulations. To study the proton conduction properties of the water wire observed at the NuoN/K interface, we performed hybrid QM/MM simulations. The QM region was described at the B3LYP/def2-SVP level (39–41), and comprised residues $E72_K$, $E133_N$, $T160_N$, $K247_N$, and eight water molecules. Starting structures were obtained from the last frame of the 250-ns unconstrained MD simulation. The water molecule closest to the N-side of the membrane was modified into a hydronium ion. The classic (MM) region was trimmed to include subunits NuoN/A/J/K, including a 3 Å water shell. This MM region was described using the CHARMM27 force field (36). Link atoms were introduced between the Cα and Cβ atoms for each residue. Five MD simulations, 5 ps each, were performed at constant temperature ($T = 310$ K) using a 1-fs timestep in Q-Chem/CHARMM (42–44).

Electrostatics Calculations. Continuum electrostatics calculations were performed using the MEAD software (45). Residues within ±7 Å of the membrane center were modeled as titratable using the following reference pK_a values in bulk: Glu: 4.0, Asp: 4.0, His: 6.5, Tyr: 9.6, Lys: 10.4, Arg: 12.0. The protein interior and a membrane slab, extending in the z direction by ±20 Å, were modeled as a low dielectric medium with a dielectric constant of $\varepsilon = 4$, whereas the surrounding solvent was modeled as a high dielectric medium with $\varepsilon = 80$. Monte Carlo sampling of the 2^N protonation states was performed with KARLSBERG (46) to obtain pK_a values.

ACKNOWLEDGMENTS. We thank the high-performance Biowulf cluster (http://biowulf.nih.gov) at the National Institutes of Health for computer time. This work was supported by the Intramural Research Program of the National Institute of Diabetes and Digestive and Kidney Diseases, National Institutes of Health (V.R.I.K. and G.H); the Max Planck Society (G.H.); a European Molecular Biology Organization Long-Term Fellowship (to V.R.I.K.); and by grants from the Sigrid Jusélius Foundation, Biocentrum Helsinki, and the Academy of Finland (all to M.W.).

1. Brandt U (2006) Energy converting NADH:quinone oxidoreductase (complex I). *Annu Rev Biochem* 75:69–92.
2. Verkhovskaya M, Bloch DA (2013) Energy-converting respiratory complex I: on the way to the molecular mechanism of the proton pump. *Int J Biochem Cell Biol* 45(2): 491–511.
3. Wikström M (1984) Two protons are pumped from the mitochondrial matrix per electron transferred between NADH and ubiquinone. *FEBS Lett* 169(2):300–304.
4. Wikström M, Hummer G (2012) Stoichiometry of proton translocation by respiratory complex I and its mechanistic implications. *Proc Natl Acad Sci USA* 109(12):4431–4436.
5. Mitchell P (1961) Coupling of phosphorylation to electron and hydrogen transfer by a chemi-osmotic type of mechanism. *Nature* 191:144–148.
6. Kensche PR, Duarte I, Huynen MA (2012) A three-dimensional topology of complex I inferred from evolutionary correlations. *BMC Struct Biol* 12:19.
7. Sazanov LA, Hinchliffe P (2006) Structure of the hydrophilic domain of respiratory complex I from *Thermus thermophilus*. *Science* 311(5766):1430–1436.
8. Verkhovskaya ML, Belevich N, Euro L, Wikström M, Verkhovsky MI (2008) Real-time electron transfer in respiratory complex I. *Proc Natl Acad Sci USA* 105(10):3763–3767.
9. Dröge W (2002) Free radicals in the physiological control of cell function. *Physiol Rev* 82(1):47–95.
10. Efremov RG, Sazanov LA (2011) Structure of the membrane domain of respiratory complex I. *Nature* 476(7361):414–420.
11. Efremov RG, Baradaran R, Sazanov LA (2010) The architecture of respiratory complex I. *Nature* 465(7297):441–445.
12. Efremov RG, Sazanov LA (2012) The coupling mechanism of respiratory complex I—A structural and evolutionary perspective. *Biochim Biophys Acta* 1817(10):1785–1795.
13. Baradaran R, Berrisford JM, Minhas GS, Sazanov LA (2013) Crystal structure of the entire respiratory complex I. *Nature* 494(7438):443–448.
14. Dröse S, et al. (2011) Functional dissection of the proton pumping modules of mitochondrial complex I. *PLoS Biol* 9(8):e1001128.
15. Stubbe J, Nocera DG, Yee CS, Chang MCY (2003) Radical initiation in the class I ribonucleotide reductase: Long-range proton-coupled electron transfer? *Chem Rev* 103(6):2167–2201.
16. Kaila VRI, Hummer G (2011) Energetics of direct and water-mediated proton-coupled electron transfer. *J Am Chem Soc* 133(47):19040–19043.
17. Friedrich T (2001) Complex I: A chimaera of a redox and conformation-driven proton pump? *J Bioenerg Biomembr* 33(3):169–177.
18. Yagi T, Matsuno-Yagi A (2003) The proton-translocating NADH-quinone oxidoreductase in the respiratory chain: The secret unlocked. *Biochemistry* 42(8):2266–2274.
19. Sazanov LA (2007) Respiratory complex I: Mechanistic and structural insights provided by the crystal structure of the hydrophilic domain. *Biochemistry* 46(9):2275–2288.
20. Euro L, Belevich G, Verkhovsky MI, Wikström M, Verkhovskaya M (2008) Conserved lysine residues of the membrane subunit NuoM are involved in energy conversion by the proton-pumping NADH:ubiquinone oxidoreductase (complex I). *Biochim Biophys Acta* 1777(9):1166–1172.
21. Ohnishi ST, Salerno JC, Ohnishi T (2010) Possible roles of two quinone molecules in direct and indirect proton pumps of bovine heart NADH-quinone oxidoreductase (complex I). *Biochim Biophys Acta* 1797(12):1891–1893.
22. Efremov RG, Sazanov LA (2011) Respiratory complex I: 'Steam engine' of the cell? *Curr Opin Struct Biol* 21(4):532–540.
23. Hunte C, Zickermann V, Brandt U (2010) Functional modules and structural basis of conformational coupling in mitochondrial complex I. *Science* 329(5990):448–451.
24. Forrest LR, et al. (2008) Mechanism for alternating access in neurotransmitter transporters. *Proc Natl Acad Sci USA* 105(30):10338–10343.
25. Kaila VRI, Verkhovsky MI, Wikström M (2010) Proton-coupled electron transfer in cytochrome oxidase. *Chem Rev* 110(12):7062–7081.
26. Kaila VRI, Verkhovsky MI, Hummer G, Wikström M (2008) Glutamic acid 242 is a valve in the proton pump of cytochrome *c* oxidase. *Proc Natl Acad Sci USA* 105(17): 6255–6259.
27. Kaila VRI, Verkhovsky MI, Hummer G, Wikström M (2009) Mechanism and energetics by which glutamic acid 242 prevents leaks in cytochrome *c* oxidase. *Biochim Biophys Acta* 1787(10):1205–1214.
28. Pomès R, Roux B (2002) Molecular mechanism of H+ conduction in the single-file water chain of the gramicidin channel. *Biophys J* 82(5):2304–2316.
29. Cao Z, et al. (2010) Mechanism of fast proton transport along one-dimensional water chains confined in carbon nanotubes. *J Am Chem Soc* 132(33):11395–11397.
30. Kaila VRI, Hummer G (2011) Energetics and dynamics of proton transfer reactions along short water wires. *Phys Chem Chem Phys* 13(29):13207–13215.
31. Amarneh B, Vik SB (2003) Mutagenesis of subunit N of the *Escherichia coli* complex I. Identification of the initiation codon and the sensitivity of mutants to decylubiquinone. *Biochemistry* 42(17):4800–4808.
32. Wikström M, Verkhovsky MI, Hummer G (2003) Water-gated mechanism of proton translocation by cytochrome c oxidase. *Biochim Biophys Acta* 1604(2):61–65.
33. Sharma V, Wikström M, Kaila VRI (2012) Dynamic water networks in cytochrome cbb3 oxidase. *Biochim Biophys Acta* 1817(5):726–734.
34. Freier E, Wolf S, Gerwert K (2011) Proton transfer via a transient linear water-molecule chain in a membrane protein. *Proc Natl Acad Sci USA* 108(28):11435–11439.
35. Li J, et al. (2013) Transient formation of water-conducting states in membrane transporters. *Proc Natl Acad Sci USA* 110(19):7696–7701.
36. MacKerell AD, Jr., et al. (1998) All-atom empirical potential for molecular modeling and dynamics studies of proteins. *J Phys Chem B* 102(18):3586–3616.
37. Phillips JC, et al. (2005) Scalable molecular dynamics with NAMD. *J Comput Chem* 26(16):1781–1802.
38. Humphrey W, Dalke A, Schulten K (1996) VMD: Visual molecular dynamics. *J Mol Graph* 14(1):33–38, 27–28.
39. Becke AD (1993) Density-functional thermochemistry. III. The role of exact exchange. *J Chem Phys* 98(7):5648–5652.
40. Lee C, Yang W, Parr RG (1988) Development of the Colle-Salvetti correlation-energy formula into a functional of the electron density. *Phys Rev B Condens Matter* 37(2): 785–789.
41. Weigend F, Ahlrichs R (2005) Balanced basis sets of split valence, triple zeta valence and quadruple zeta valence quality for H to Rn: Design and assessment of accuracy. *Phys Chem Chem Phys* 7(18):3297–3305.
42. Shao Y, et al. (2006) Advances in methods and algorithms in a modern quantum chemistry program package. *Phys Chem Chem Phys* 8(27):3172–3191.
43. Brooks BR, et al. (2009) CHARMM: The biomolecular simulation program. *J Comput Chem* 30(10):1545–1614.
44. Woodcock HL, 3rd, et al. (2007) Interfacing Q-Chem and CHARMM to perform QM/MM reaction path calculations. *J Comput Chem* 28(9):1485–1502.
45. Bashford D, Gerwert K (1992) Electrostatic calculations of the pK_a values of ionizable groups in bacteriorhodopsin. *J Mol Biol* 224(2):473–486.
46. Rabenstein B, Knapp EW (2001) Calculated pH-dependent population and protonation of carbon-monoxy-myoglobin conformers. *Biophys J* 80(3):1141–1150.